Investigations of Physical Processes in Solar Flare Plasma on the Basis of RESIK Spectrometer Observations

Z. Kordylewski, J. Sylwester, B. Sylwester, A. Kępa, M. Kowaliński, and W. Trzebiński

X-ray spectroscopy generally uses the data obtained with the help of spectrometers with crystals, acting as dispersive elements. According to Bragg's law, the wavelength λ of X-radiation, reflected from the crystal, depends on θ incidence angle. This dependence is presented as

$$k\lambda = 2d \sin\theta,$$

where k is the order of reflection and d is the crystal lattice spacing. The change of angle of incidence of radiation at the crystal causes the X-ray spectrum is formed within the wavelengths range corresponding to the extreme values of crystal rotational change.

The X-ray spectrometers with the flat crystals have one deficiency, especially when they are used for observations of solar flare spectra. To obtain the spectrum through scanning with incidence angle change, some time is required—usually even few minutes. This complicates the interpretation of the obtained spectra for quickly varying radiation sources, such as solar flares. The obtained spectra are not homogeneous—individual parts are irradiated by plasma having various physical characteristics. This is caused by variation of physical conditions during the scanning.

Simultaneous registration of spectra of quickly varying sources may be obtained through the use of curved fixed crystals instead of the scanning flat crystals spectrometer. Illuminating such a curved crystal with parallel X-ray beam allows to obtain, after the reflection, the whole spectrum covering certain wavelengths range, as the incidence angle at curved crystal surface represents a monotonous function of incidence point position measured along the crystal. On the other hand, the spectrum registration becomes more complicated, as it requires the use of

Z. Kordylewski · J. Sylwester (✉) · B. Sylwester · A. Kępa · M. Kowaliński · W. Trzebiński
Space Research Centre of Polish Academy of Sciences (SRC PAS), Wrocław, Poland
e-mail: js@cbk.pan.wroc.pl

V. Kuznetsov (ed.), *The Coronas-F Space Mission*, Astrophysics and Space Science Library 400, DOI 10.1007/978-3-642-39268-9_6,

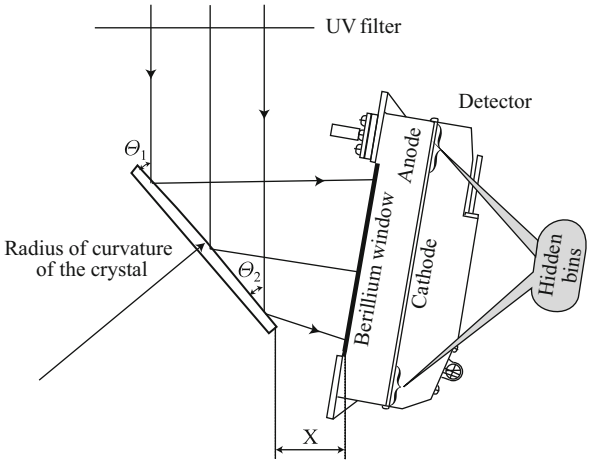

Fig. 1 The scheme of spectrometer with bent crystals, used in RESIK experiment. The parallel rays bundle falls into the surface of cylindrically curved crystal (with indicated radius). The incidence angle smoothly changes along the crystal. As a result the single points on detector window are illuminated by radiation with different wavelengths, thus forming the X-ray spectrum. From [21]

so-called X-ray position sensitive detector. Such detector should be fitted with a known function of the detection of line coordinate of the points (along the dispersion direction), on which the radiation photons fall. In the same manner it is possible to measure simultaneously the radiation intensity in separate wavelengths. The scheme of the spectrometer with curved crystals is shown in Fig. 1.

Starting from the 1980s of the last century the Solar Physics Division of the Space Research Center of Polish Academy of Sciences in Wrocław conducted the works with X-ray spectrometers for the investigation of radiation of the Sun. The works with Polish spectrometers, which have been started on Vertical-8 and Vertical-9 geophysical rockets [12], were continued with so-called Dopplerometer spectrometers on Vertical-11 rocket [13] and CORONAS-I satellite [14], and have lead to the construction of RESIK spectrometer with bent crystals at CORONAS-F spacecraft [21]. During the design of RESIK instrument, the similar spectrometer BCS was used as a model. Such spectrometer operated on Yohkoh satellite [2]. The RESIK instrument design was performed jointly by the groups of experts of Naval Research Laboratory (NRL, USA), Rutherford Appleton Laboratory (RAL), and Mullard Space Science Laboratory (MSSL, UK). The works were also supported by scientists of Pushkov Institute of Terrestrial Magnetism, Ionosphere and Radio Waves Propagation of the Russian Academy of Sciences. General works supervision was executed by Solar Physics Division of the Space Research Center of Polish Academy of Sciences.

The RESIK spectrometer, shown in Fig. 2, consisted of two sections (A and B), closed in one unit, designed for operation on instrumental platform located outside the sealed satellite container. The electronic unit, which included the computer, was located inside the sealed CORONAS-F satellite container. In each of A and B sections of the spectrometer two crystals were used as dispersive elements—they were made of silicon (Si) and quartz (Qu) single crystals wafers. The application of materials with a low atomic number Z helped to reduce the fluorescence effects, which, as is known, are proportional to Z^4 of the crystal material. Undesirable fluorescence radiation appears as a result of illumination of crystals with solar

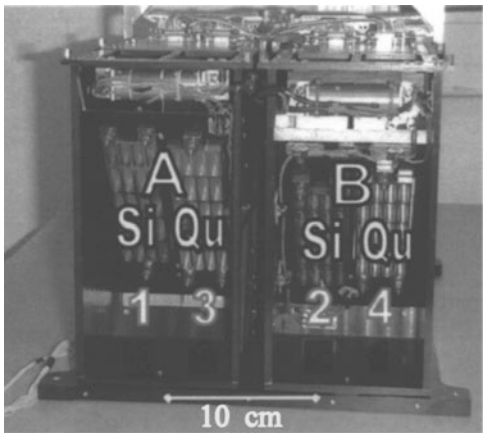

Fig. 2 The general view of RESIK spectrometer (without the cover) from the side of crystals support system. The figure contains the indications of sections A and B, crystal material, and spectrometer channels numbers. From [21]

radiation. The crystals, used in RESIK, have been manufactured, curved, and calibrated at the USA National Institute of Standards and Technology (NIST).

After the diffraction on crystals the X-radiation was registered by two linear double proportional detectors, manufactured according to those used in BCS device on Yohkoh satellite. In each of A and B sections of RESIK spectrometer there was one double detector with input window made of beryllium foil of 125 μm thickness. Each one of these detectors measured the radiation reflected separately by quartz and silicon crystals. The split of signals from two channels was performed in the counter with application of two anodes with the high voltage (power 1.5 kV), connected to preamplifier. The position of points of incidence of radiation at the window of the detector, defined in 256 bins, came out from the relationship of signal charges recorded from two parts of wedge and wedge cathode, located directly behind the anode. Due to small radius of curvature of applied crystals the spectral dispersion amounted to 0.02–0.04 Å/bin. These values are slightly higher than natural widths of spectral lines and represent instrumental width. The calibration of detectors with the use of ^{55}Fe radioisotope source pulled out to the counters field of view was performed several times in course of the flight. The spare elements (detectors, high voltage sources, and electronic boards for detector signals processing) which remained after the BCS experiment at Yohkoh satellite were used in RESIK equipment.

The correct selection of crystal materials, their curvature radiuses, and optimal relative position of crystals and detectors inside the device has ensured the obtainment of nearly complete spectral coverage in a wide range, from 3.3 to 6.1 Å. Such range is especially valuable for analysis of elemental abundance of solar plasma. It includes the lines of elements with high and low first ionization potential (FIP). In particular, the spectra obtained by RESIK show the emission lines of the following elements: Ar (FIP = 15.8 eV), S (FIP = 10.4 eV), Si (FIP = 8.2 eV), and K (FIP = 4.6 eV). The detailed characteristics of four channels of RESIK spectrometer are presented in Table 1.

Table 1 RESIK spectrometer parameters

		Channel 1	Channel 2	Channel 3	Channel 4
Detector		A	B	A	B
Crystal		Si	Si	Quartz	Quartz
Plane		(111)	(111)	$(10\bar{1}0)$	$(10\bar{1}0)$
$2d$ spacing (Å)		6.27	6.27	8.51	8.51
Bent radius (cm)		110.0	100.0	145.0	52.5
Length (cm)		12.8	11.6	12.8	12.8
Detector edge to crystal edge distance[a] (cm)		3.74	4.66	4.12	4.75
Incidence angle range (°)		29.5–39.7	35.0–44.9	28.2–36.6	31.7–48.2
Rc-integrated reflectivity[b] (μrad)		53	52	21	18
Wavelength[c] (Å)	Nominal range	3.40–3.80	3.83–4.27	4.35–4.86	5.00–6.05
	Extreme range	3.33–3.90	3.78–4.32	4.23–4.92	4.90–6.15
Wavelength resolution (mÅ)		8	9	12	17
Dispersion[b] (mÅ bin^{-1})		2.49	2.28	2.85	4.99
Principal lines in range		Ar XVIII, K XVIII	Ar XVII, S XV	S XVI	S XV, Si XIV, Si XIII

[a] Minimum distance between the crystal and detector measured along the line perpendicular to the direction of the source

[b] The values of reflection coefficient and the dispersion are given for the first-order reflection in the central part of the crystal

[c] Nominal range—for the radiation beam parallel to the optical axis of the instrument; maximum range—including the beams as inclined to the optical axis (slope angle is comparable with the angular radius of the Sun)

Owing to unprecedented sensitivity of RESIK spectrometer it became possible to make measurements not only of strong solar flares but also of the weak ones. The instrument used a dynamical method of on board adjustment of signal accumulation time (DGI). The RESIK on board computer analyzed the level of emission of observed X-radiation of the Sun and automatically matched the optimal DGI accumulation time. Thus, in the rise phase of a strong flare DGI time could amount to 5 min at the very beginning of the flare, decreasing to 1 s at maximum of the event.

The RESIK device operated successfully in a flight for almost 2 years. This period may be divided in several stages. After the initial control phase lasting for a short period in middle October 2001, the work activation was performed on August 24, 2001, and lasted till October 7, 2001. At this time period, on August 25,

2001, a very strong flare has occurred on the Sun. The analysis of first observations has shown the need for improvement of RESIK on board operation program. The power supply was henceforth disconnected from the device for the duration of improvement works, to protect the detector performance from deterioration. At the end of January and beginning of February 2002, the power supply was restored, and the device operated uninterruptedly till May 22, 2003. During the device active measurement phase the parameters of device operation have been changed several times upon the ground commands, in order to obtain the best possible results of observation. The optimal parameters have been matched at the end of December 2002. Starting from that date the most valuable material for many flares has been gathered, including the data for 14 phenomena (January–March 2003; middle level of solar activity), for which the average spectrum is shown in Fig. 3. The RESIK instrument has recorded nearly one million of X-ray spectra. Observation catalogue is accessible at the web site http://www.cbk.pan.wroc.pl/resik_catalogue.htm.

In course of the processing of observed spectra several factors were considered. One of them was the "notch" effect (FPS), which gives artificial peaks in spectra as a result of division of integer numbers which defined the positions of photons measured along the detector length. Another important fact in data processing was the correct accommodation of the results of ground calibration and in-flight calibrations with the use of ^{55}Fe radioisotope. Many efforts were needed to eliminate the crystals fluorescence effect, caused by radiation of the Sun. This radiation contributed to the observed continuum level. This effect could be partially reduced by matching the relevant device operation parameters, while the remaining part of its impact could be eliminated by computational method only. It required the knowledge of detectors laboratory calibration parameters, as well as performance of special sequences of device operation taken in flight. Such actions required 34 h of measurements, which have been performed from August 30 to September 5, 2002.

The obtained spectra in 3.3–6.1 Å range are especially interesting, as in this wavelength range they have been observed for the first time with such high sensitivity and spectral resolution. Moreover, owing to the accurate calibration of the device in the laboratory (performed at RAL, MSSL) and during the flight, it was possible to reduce the observation and obtain the absolute error level not exceeding 20 %. Figure 3 shows the spectra from all four RESIK spectrometer channels, averaged for 14 flares of different classes. These averaged spectra have been obtained by summation of several tens of individual registrations covering the rise, maximum, and decay phase of the flares. The summation was performed with the purpose of increasing the statistics and revealing all spectral features characteristics for hot and cooler plasma.

The RESIK spectrometer measured the spectra in a wide intensity range, which covers four orders of magnitude. It allowed to obtain the spectra not only for maximum phases of strong flares, but also for their growth and decay phases, and even for quiet corona. The possible examples are the observations of a strong solar limb flare on January 21, 2003. This flare lasted almost 5 h and has reached M1.9 level according to GOES class. Figure 4 illustrates two solar spectra—one (on the left), for quiet solar conditions, has been obtained 5 h before the maximum of the

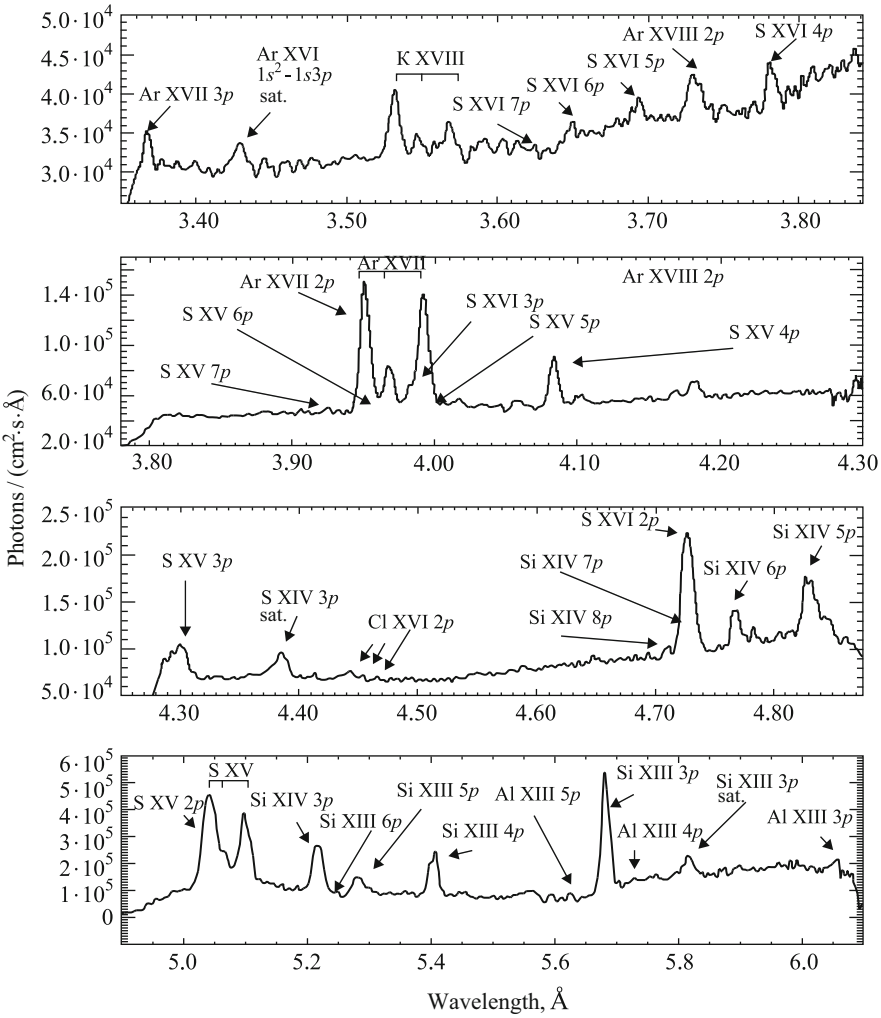

Fig. 3 Averaged spectra of 14 flares observed in the period January–March 2003. The spectra have been obtained in four channels of RESIK spectrometer (the wavelength range 3.35–6.05 Å). The figure shows identification of lines—many of them have been observed in astrophysical plasma for the first time. From [6]

flare, the second one (on the right) corresponds to the flare rise phase. The difference between these spectra is clearly seen. It is caused not only by the growth of general intensity level, but also by the presence of different individual spectral lines and their varying intensities. For example, the helium-like Ar XVII ($\lambda \approx 3.95$ Å) triplet has a high intensity only during the flare development. The thin solid line below the spectra shows the continuum radiation level calculated using CHIANTI atomic code. The calculations have been performed with the use of characteristic

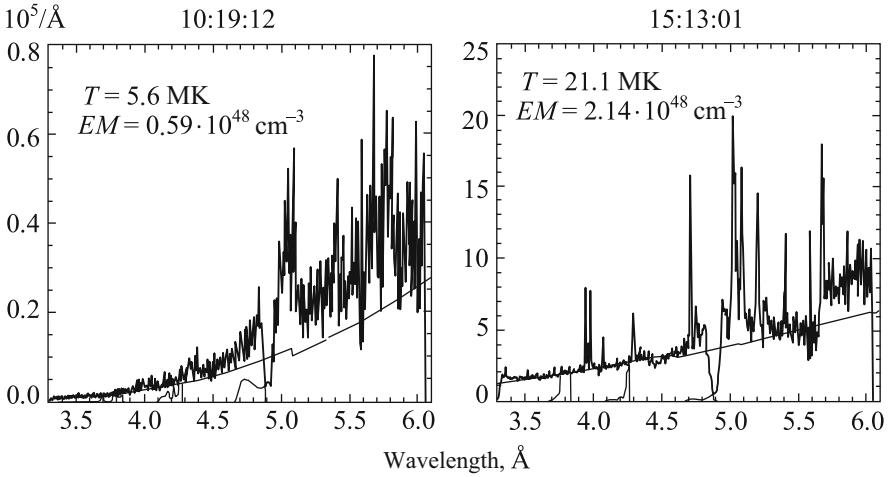

Fig. 4 Comparison of spectra obtained by RESIK on January 21, 2003, in the conditions of quiet Sun (on the *left*) and during M1.9 class flare (on the *right*). The *thin line* below the spectra shows the level of continuous radiation, calculated with CHIANTI code for temperature and emission measure, indicated in the drawing. The spectra vary significantly in terms of intensity and ratios of the intensities in individual spectral lines. From [22]

parameters of plasma source (temperature T and emission measure EM), indicated in the figure. These parameters have been determined based on ratio of fluxes in the first and fourth RESIK spectrometer channels, with the assumption that radiating plasma is isothermal. The time dependence of intensity changes recorded in a number of well-seen spectral lines is shown in Fig. 5. For clarity the zero levels of every curve have been vertically shifted in a manner to prevent their overlapping. It may be seen that while the radiation in "hot" lines decays faster (e.g., Ar XVIII, Ar XVII, K XVIII), it decays much slower in the lines formed in cooler plasma.

During ground calibration of the spectrometer, the accurate spectral reference wavelength scale has been established. The numerical model of every device sections has been applied in this respect. The accuracy of determination of incident positions along the detector and crystals in this model is better than 0.1 mm. The wavelengths scale accuracy is determined by such factors as crystal curvature radius, relative position of crystal and detector window, and linearity of electronic system against the photon incidence position. One of the most important physical factors influencing the wavelength scale accuracy is the inclination of emission source relative to diffraction plane. Depending on the position of active region or flare on the Sun, the observed positions of lines may move for several bins along the detector anode length.

The precise wavelength calibration as well knowledge of orientation of satellite axis relative to the center of the disc of the Sun has allowed the determinations of wavelengths of single spectral lines with accuracy of ∼0.001 Å. It made possible to compare the values of wavelengths of observed lines with the data calculated

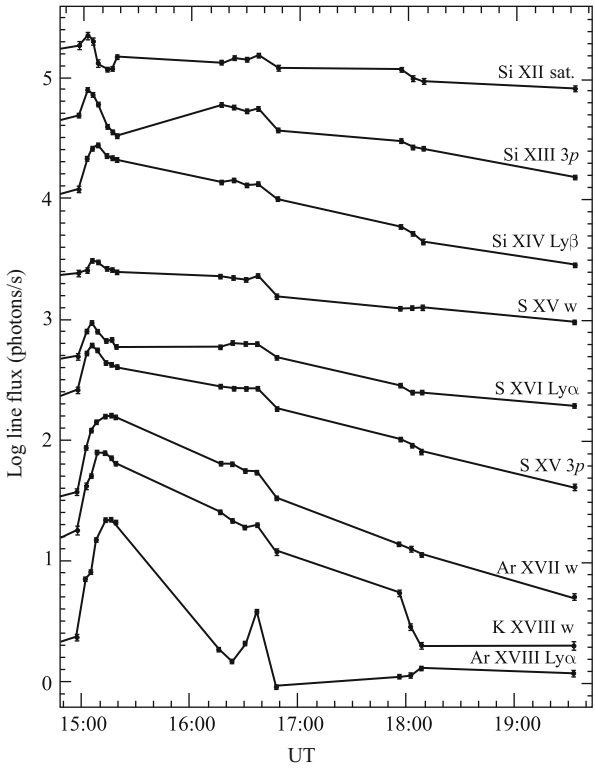

Fig. 5 Time variations of fluxes in individual spectral lines, observed in RESIK spectra during the flare of January 21, 2003. This flare of M1.9 class occurred at the limb of the Sun. Individual curves are vertically shifted in order to increase visibility. From [22]

theoretically from atomic physics. The good coincidence of wavelengths between the two is the base for identification of new spectral features, presented in Fig. 3. The observed spectrum contains the lines corresponding to principal resonance transitions in hydrogen-like ions of Al, Si, S, and Ar and helium-like ions of Si, S, Cl, Ar, and K. The special achievement was identification for the first time of the new chlorine [20] and potassium [9] lines. The complete list of identified spectral lines is specified in Table 2 (for the first reflection order) and Table 3 (for the third reflection order). The table specifies the wavelength, temperature at maximum of emission function, the responsible ion, and relevant transition.

The obtained spectra show the lines corresponding to the transitions to low excited levels $n = 2$, which have been observed previously, and to high ones, $n = 10$, which have not been previously observed in the astrophysical plasmas. Moreover, the spectra show the forbidden and intercombination lines, corresponding to helium-like ions, as well as multiple satellites formed in the processes of dielectronic recombination and excitation of inner shell electrons. The values of relative intensities of lines of higher components of line series, for unknown reasons, are higher than theoretically predicted values for thermal plasma [6].

In the course of processing of spectra it appeared that the ratio of intensity of pair of Si lines (satellite line $\lambda = 5.82$ Å and resonance line $\lambda = 5.68$ Å), which are

Table 2 The principal emission lines observed in the first reflection order spectra

Number	λ (Å)	T (MK)	Ion	Transition
1	3.36	22	Ar XVII	$1s^2\ ^1S_0$–$1s3p\ ^{1,3}P_1$
2	3.43	19	Ar XVI	Satellite to [1]
3	3.53	26	K XVIII	$1s^2\ ^1S_0$–$1s2p\ ^1P_1$
4	3.57	19	K XVIII	$1s^2\ ^1S_0$–$1s2s\ ^3S_1$
5	3.59	17	K XVII	Satellite to [3]
6	3.70	26	S XVI	$1s\ ^2S_{1/2}$–$5p\ ^2P_{3/2,1/2}$
7	3.74	36	Ar XVIII	$1s\ ^2S_{1/2}$–$2p\ ^2P_{3/2,1/2}$
8	3.79	26	S XVI	$1s\ ^2S_{1/2}$–$4p\ ^2P_{3/2,1/2}$
9	3.95	22	Ar XVII	$1s^2\ ^1S_0$–$1s2p\ ^1P_1$
10	3.97	22	Ar XVII	$1s^2\ ^1S_0$–$1s2p\ ^3P_{1,2}$ $(x+y)$
11	3.99	22	Ar XVII	$1s^2\ ^1S_0$–$1s2s\ ^3S_1$
12	4.02		?	
13	4.09	16	S XV	$1s^2\ ^1S_0$–$1s4p\ ^1P_1$
14	4.10	14	S XIV	Satellite to $1s^2\ ^1S_0$–$1s5p\ ^1P_1$
15	4.18	35	Cl XVII	$1s\ ^2S_{1/2}$–$2p\ ^2P_{3/2,1/2}$
16	4.30	15	S XV	$1s^2\ ^1S_0$–$1s3p\ ^1P_1$
17	4.39	14	S XIV	Satellite to [16]
18	4.44	19	Cl XVI	$1s^2\ ^1S_0$–$1s2p\ ^1P_1$
19	4.73	24	S XVI	$1s\ ^2S_{1/2}$–$2p\ ^2P_{3/2,1/2}$
20	4.77		?	
21	4.83	14	Si XIV	$1s\ ^2S_{1/2}$–$5p\ ^2P_{3/2,1/2}$
22	4.96	24	Si XIV	$1s\ ^2S_{1/2}$–$4p\ ^2P_{3/2,1/2}$
23	5.04	13	S XV	$1s^2\ ^1S_0$–$1s2p\ ^1P_1$)
24	5.10	14	S XV	$1s^2\ ^1S_0$–$1s2s\ ^3S_1$)
25	5.22	14	Si XIV	$1s\ ^2S_{1/2}$–$3p\ ^2P_{3/2,1/2}$
26	5.28	15	Si XIII	$1s^2\ ^1S_0$–$1s5p\ ^1P_1$
27	5.40	11	Si XIII	$1s^2\ ^1S_0$–$1s4p\ ^1P_1$
28	5.59		?	
29	5.68	10	Si XIII	$1s^2\ ^1S_0$–$1s3p\ ^1P_1$
30	5.82	7	Si XII	Satellite to [29]
31	5.87		?	

clearly distinguished from the background, is a good indicator of the temperature of plasma, representing conditions in the quiet corona. The intensity ratio of these two lines decreases by an order of magnitude when plasma temperature increases from 3 to 10 MK [10]. It was predicted by the theory, but was for the first time observed on RESIK spectra. Sometimes the observed intensity of satellite line is higher than theoretical value for thermal plasma, which may evidence the existence of additional non-thermal processes contributing to satellite lines formation.

The solar plasma, besides the temperature T, is also characterized by so-called emission measure $\mathrm{EM} = N^2V$, which, with the assumption of constant volume V of the flare during the evolutions, gives the density N of radiating plasma. Another important characteristic parameter for radiating plasma is the so-called thermodynamic measure $\mathrm{ThM} = T \times (\mathrm{EM})^{1/2}$ [18], which is linearly related to the

Table 3 The principal emission lines observed in the third reflection order spectra

Number	λ (Å)	T (MK)	Ion	Transition
1	1.457		?	
2	1.542	180	Ni XXVIII	$1s\ ^2S_{1/2}–2p\ ^2P_{3/2,1/2}$
3	1.571	60	Fe XXV	$1s^2\ ^1S_0–1s3p\ ^1P_1$
4	1.591	80	Ni XXVII	$1s^2\ ^1S_0–1s2p\ ^1P_1$
5	1.750		Fe K β	
6	1.781	150	Fe XXVI	$1s\ ^2S_{1/2}–2p\ ^2P_{3/2,1/2}$
7	1.850	54	Fe XXV	$1s^2\ ^1S_0–1s2p\ ^1P_1$
8	1.910	30	Fe	Multiple satellites
9	1.980		?	
10	2.025		?	

amount of thermal energy of the flare plasma. The average values of T and EM for the above-mentioned strong flare of January 21, 2003, were determined for 17 time intervals based on the ratios of total fluxes (including the continuous radiation and spectral lines) measured in two adjacent channels of RESIK spectrometer. The theoretical spectrum calculated with the application of CHIANTI code was used [3]. The comparison of time dependence of thermodynamic measure ThM and temperature T shows that ThM maximum occurs 10 min later than observed maximum of plasma temperature T.

In the research works [5, 11, 17] was indicated that it is convenient to use the so-called diagnostic diagram (DD) for the investigation of energy release and cooling plasmas. In fact DD represents the temperature–density diagram. Figure 6 represents such a diagram for the analyzed flare; the diagram shows two theoretical straight lines: the first one (OFF), with inclination 2, corresponds to evolution in case of sudden switched-off of plasma heating in the flare, the second one (QSS), with inclination 1/2, corresponds to quasi-steady evolution with gradually decreasing heating. The zigzag line between OFF and QSS lines links the observation points. For flare decay phase it is located along the straight line with inclination $\sim$1.1. It indicates that during flare decay phase the significant heating of plasma was still operating.

Many interpretations in the area of solar plasma diagnostics use the so-called one-temperature model. The heavy line in Fig. 7 shows a small interval of spectrum in the range 5–6 Å, obtained by averaging of observations for nine selected flares, which occurred at the beginning of 2003 (from January to March). The thin line shows the theoretical spectrum calculated with CHIANTI code. The applied values of temperature T and emission measure EM have been obtained in one-temperature approximation from the ratios of fluxes in the first (3.3–3.8 Å) and second (3.8–4.3 Å) spectral channels of RESIK instrument. As these two spectra do not coincide, the theoretical calculation has been repeated for T and EM values, obtained from the ratios of fluxes of lines, sensitive to the temperature (shaded in black) [10]. In this case the calculated spectrum (light gray curve) and observed

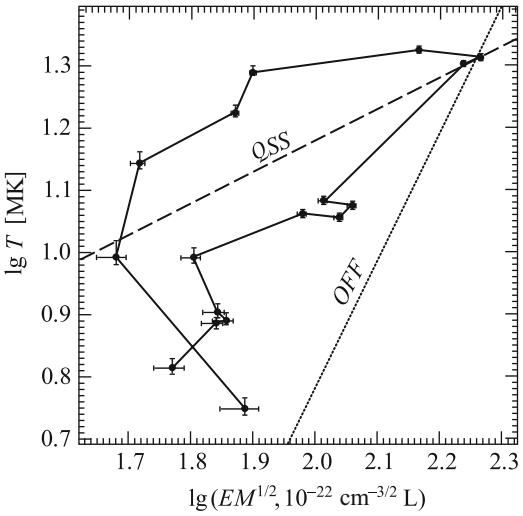

Fig. 6 Diagnostic diagram (DD) for the flare on January 21, 2003. The location of points obtained from observations in relation to theoretical straight lines QSS (quasi-steady evolution) and OFF (sudden switched-off) defines the character of flare heating evolution. The *zigzag line* between QSS and OFF evidences the energy release in the flare, even during the phase of its late decay. From [22]

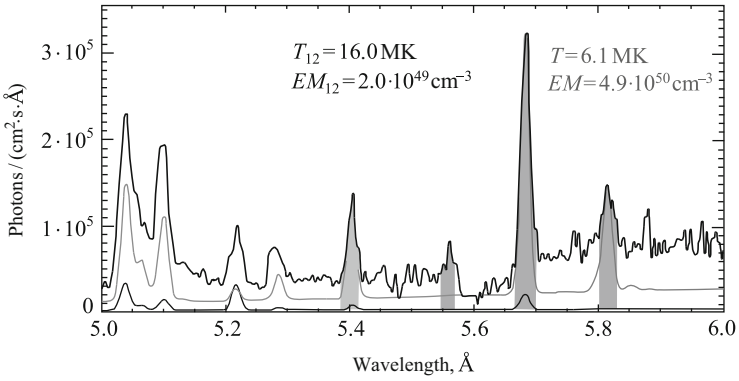

Fig. 7 The fragment of spectrum (*heavy line*) averaged upon the observations of nine flares. The *thin lines* show the theoretical spectra, calculated with CHIANTI code for indicated parameters of emitting plasma. The disagreement between the theoretical curves and observations evidences the presence of multi-temperature plasma in the flares. From [22]

spectrum also did not coincide. These discrepancies indicate that radiating plasma is multi-temperature. It may be also seen that not all observed lines have their counterparts in the theory spectra calculated using CHIANTI code.

Table 4 The spectral lines used for DEM(T) calculations

Number	Wavelength ranges (Å)	Main lines
1	3.340–3.368	Ar XVII $1s^2\ ^1S_0$–$1s3p\ ^1P_1$
2	3.688–3.699	S XVI $1s\ ^2S_{1/2}$–$5p\ ^2P_1$
3	3.724–3.740	Ar XVIII $1s\ ^2S_{1/2}$–$2p\ ^2P_{1/2,3/2}$
4	3.777–3.789	S XVI $1s\ ^2S_{1/2}$–$4p\ ^2P_{1/2,3/2}$
5	3.944–3.962	Ar XVII $1s^2\ ^1S_0$–$1s2p\ ^1P_1$ (w)
6	3.963–3.980	Ar XVII $1s^2\ ^1S_0$–$1s2p\ ^3P_{1,2}$ (x+y)
7	3.981–4.004	Ar XVII $1s^2\ ^1S_0$–$1s2s\ ^3S_1$ (z)
8	4.076–4.091	S XV $1s^2\ ^1S_0$–$1s4p\ ^1P_1$
9	4.288–4.315	S XV $1s^2\ ^1S_0$–$1s3p\ ^1P_1$
10	4.720–4.743	S XVI $1s\ ^2S_{1/2}$–$2p\ ^2P_{1/2,3/2}$ (Lyα)
11	5.030–5.061	S XV $1s^2\ ^1S_0$–$1s2p\ ^1P_1$ (w)
12	5.086–5.124	S XV $1s^2\ ^1S_0$–$1s2s\ ^3S_1$ (z)
13	5.204–5.232	Si XIV $1s\ ^2S_{1/2}$–$3p\ ^2P_{1/2,3/2}$ (Lyβ)
14	5.267–5.290	Si XIII $1s^2\ ^1S_0$–$1s5p\ ^1P_1$
15	5.396–5.417	Si XIII $1s^2\ ^1S_0$–$1s4p\ ^1P_1$
16	5.669–5.697	Si XIII $1s^2\ ^1S_0$–$1s3p\ ^1P_1$

For the purpose of detailed study of distribution of solar flare plasma with temperature, it is convenient to use the differential emission measure (DEM), which is described by the relation

$$\varphi(T) = \frac{N^2 dV}{dT},$$

where T, N, and V are, respectively, the temperature, density, and volume of plasma in a flare. The $\varphi(T)$ distribution shows how much of the emitting plasma is characterized with given temperature T. DEM distribution characterizes actual physical conditions in plasma. The data collected by RESIK spectrometer are suitable for DEM distribution analysis, as they contain information about the fluxes of continuous radiation and fluxes of many spectral lines in range 3.2–6.1 Å, which are formed in different temperatures. Using the data for absolute calibration of RESIK device, the fluxes in 16 strong, well-visible lines have been determined. The list of these lines is shown in Table 4. On the basis of the observed fluxes in these lines, the distribution of DEM with the temperature for many flares in different evolutionary phases has been calculated. In fact, the fluxes in lines and the underlying continuum have been used. The iteration algorithm of Withbroe–Sylwester [15] was applied for calculations. The theoretical emission functions for the line and continuum have been calculated using CHIANTI code.

The example of DEM analysis is that performed for the strong flare of M1.9 class on January 21, 2003 at 15:26 UT. The DEM shapes for several phases of flare evolution are shown in Fig. 8. It may be seen that during the whole flare evolution the general shape of distribution may be considered as two-component. These components are clearly separated: the cold plasma with temperature of 5–8 MK and

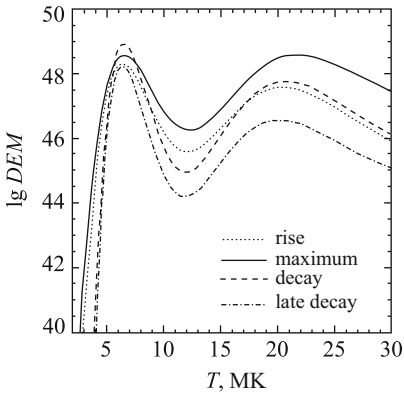

Fig. 8 The distribution of differential emission measure (DEM) for the limb long-lasting flare on January 21, 2003 at 15:26 UT (M1.9 class). Each individual *curve* corresponds to various phases of flare development. It may be seen that at every evolutionary phase the flare contained both cold and hot plasmas. From [22]

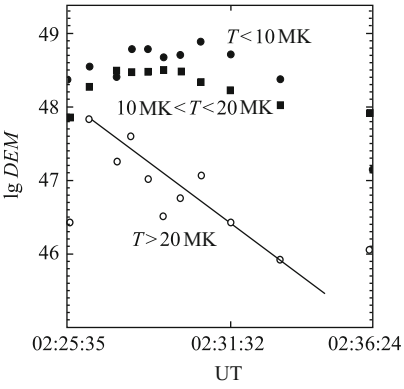

Fig. 9 Time variations of the amount of plasma at various temperatures. The calculations were performed for the flare of January 21, 2003 at 02:28 UT (C8.1 class). The behavior of hottest component differs significantly from other components. From [7]

hot one with temperature of 18–25 MK. The cold component plasma temperature is almost constant in course of the flare; however, the amount of this plasma is subject to substantial changes. During the decay phase the amount of cold plasma is almost an order of magnitude larger than that of hot one. The amount of hot plasma in course of decay decreases much more (by two orders of magnitude), while the temperature maximum of this component drops from 22 MK at there maximum to 20 MK 3 h later.

The similar DEM distributions have been obtained also for other, weaker, and faster-evolving flares. In particular, there have been performed another calculations of DEM distribution for C8.1 class flare, which occurred on January 21, 2003 at 02:28 UT and lasted only 10 min. To obtain information about the time dependence of behavior of individual DEM components, three plasma component have been identified: the cold plasma with temperature $T < 10$ MK, the component with moderate temperature 10–20 MK, and hot plasma, with temperature above 20 MK. Figure 9 illustrates the time dependence of emission measure (amounts of plasma) in these separate temperature ranges. The hot component emission measure is monotonically decreasing almost from the very beginning of flare. The amount of cooler plasma is changing weakly with time.

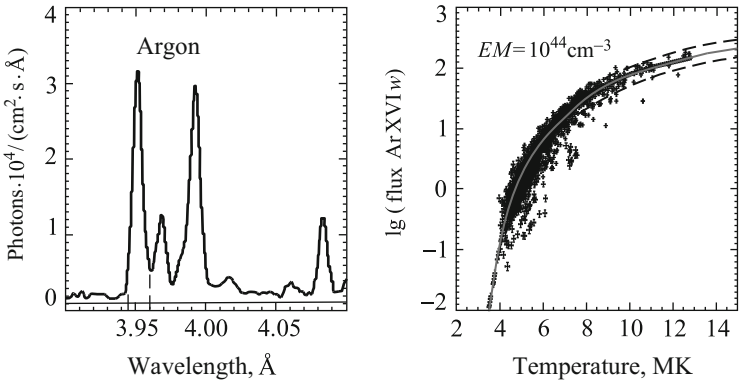

Fig. 10 On the *left*: the fragment of spectrum obtained by summation of ∼1,200 spectra of flares observed by RESIK instrument at the beginning of 2003. The spectrum involves the triplet of helium-like ion Ar XVII. On the base of observations of the fluxes of strong line *w* of this triplet ($\lambda = 3.95$ Å) the dependence flux-temperature has been obtained, as seen on the *right*. The points are the values determined from observations, the *solid line*—theoretical dependence for ionization equilibrium and average coronal abundance of argon. The *upper* and *lower dashed lines* correspond to calculations for argon abundance, two times more and two times less than the average value respectively

The spectra obtained by RESIK instrument, besides spectral lines, also show clearly the continuous radiation, which is formed in free–free and recombination processes. The level of signal, measured by RESIK spectrometer in the continuum, exceeds significantly (up 100 times) the level of orbital noise. This allows to use the continuum in the analysis of physical parameters of radiating plasma. Thus, the measured relation of intensity of the lines to the level of adjacent continuum allows to determine directly the absolute (in relation to hydrogen) abundances of elements present in hot flaring plasma.

Determination of chemical composition based on the analysis of spectra, obtained by RESIK, leads to the conclusion that the abundance of elements with low first ionization potential (FIP $<$ 10 eV) in flare plasma is higher than abundances characteristic for the photospheric plasma. So far this fact was known from spectral observations only for potassium [16, 19]. The accuracy of obtained results is evidenced by the data presented in Fig. 10. At the left there is a section of spectrum obtained through summation of multitude (∼1,200) of spectra, recorded during 400 h of observations, performed by the spectrometer from January to March 2003. This spectrum involves the triplet of argon Ar XVII helium-like ion, with resonance line *w* corresponding to $1s^2$–$1s2p$ transition. Based on the ratios of total fluxes measured in spectrometer first and fourth channels for these 1,200 spectra there were determined temperature T and total emission measure EM for every spectrum. These parameters have formed a base for the calculation of continuous radiation and normalization for unit emission measure of fluxes observed in argon triplet lines. By dividing the line emission by corresponding emission measure, this allowed to

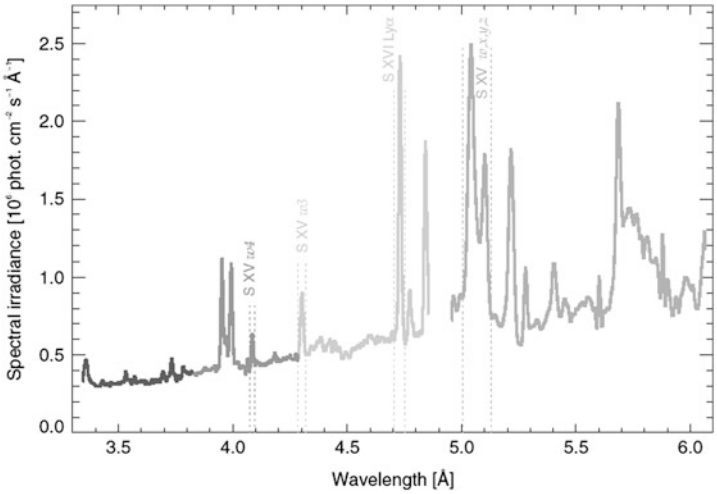

Fig. 11 Complete RESIK spectrum (channels 1–4) taken during the M4.9 flare on 2003 January 7 over the period 23:29:00–23:32:35 UT. The principal S lines used in the analysis are indicated, with *vertical dashed lines* to show the interval over which the line fluxes were estimated. From [24]

accommodate the dependence of flux in a spectral line on the amount of plasma in the source. The dependence of thus normalized line flux on the temperature is shown at the right part of Fig. 10. The points correspond to individual spectra of flares and non-flaring active regions, measured at different physical conditions on the Sun. It may be seen that the points proceed along the characteristic curve. Three continuous lines presented in the figure have been obtained theoretically for ionization equilibrium [8] and assuming three various values of argon abundance: 5.64×10^{-6} (upper), 2.82×10^{-6} (medium-solid), and 1.41×10^{-6} (lower-dashed line).

Using a similar spectroscopic method we determined the abundances of other elements for which the lines have been identified on RESIK spectra. In Fig. 11 the complete spectrum for the M4.9 flare on 2003 January 7 integrated over the 215 s is shown.

Different shades of gray indicate for the individual RESIK channels. The principal lines of the H- and He-like ions (S XVI and S XV) are noted and vertical dashed lines limit the wavelength intervals over which the line fluxes were estimated. For the sulfur abundance determinations we have used S XV *w4* line in the range 4.075–4.095 Å, S XV *w3* line in the range 4.285–4.320 Å, triplet (*w*, *x*, *y*, *z*) of S XV ion in the range 5.006–5.14 Å, and Ly-α of S XVI ion in the range 4.717–4.745 Å. The 1,448 spectra for 13 flares observed in 2003 have been used. As the most reliable we consider the value $A(\mathrm{S}) = 7.16 \pm 0.17$ (on a logarithmic scale with $H = 12$) as determined from *w4* line analysis ($1s^2$–$1s4p$ transition in S XV ion) seen in channel 2 of RESIK. In Fig. 12 the respective comparison of observations and theory is presented.

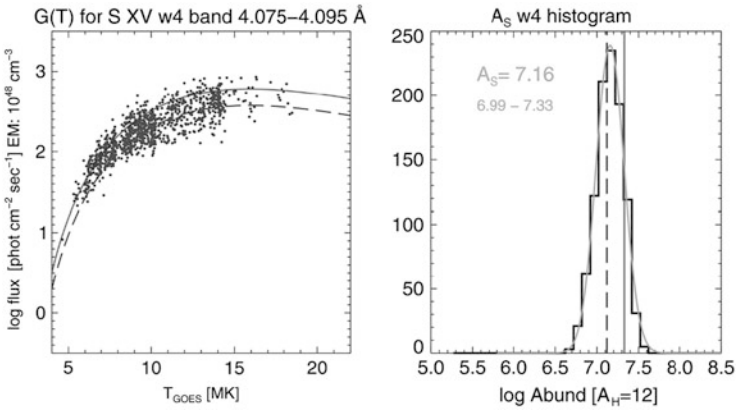

Fig. 12 *Left panel*: measured S XV *w4* line emission (in RESIK channel 2 range 4.075–4.095 Å) divided by emission measure plotted against T. The *dashed curve* is the theoretical $G(T)$ function for the photospheric S abundance ($A(\mathrm{S}) = 7.12$ [1]), the *solid curve* is for a nominal coronal abundance ($A(\mathrm{S}) = 7.33$ [4]). *Right panel*: distribution of abundance determinations with best-fit Gaussian curve. From the peak and width of the Gaussian, the S abundance is determined to be $A(\mathrm{S}) = 7.16 \pm 0.14$. The *vertical dashed* and *solid lines* correspond to the photospheric and coronal abundance, respectively. From [24]

In the left panel the measured S XV *w4* line flux divided by the emission measure is displayed for each individual spectrum vs. the isothermal temperature T. The dashed curve is the theoretical $G(T)$ function for the photospheric S abundance $A(\mathrm{S}) = 7.12$ while the solid curve is for a nominal coronal abundance $A(\mathrm{S}) = 7.33$. In the right panel the distribution of S abundance determinations with the best fit Gaussian curve is shown. From the peak and width of the Gaussian, the value of S abundance and error limits are determined. The vertical dashed and solid red lines correspond to the photospheric and coronal abundances, respectively. Estimates from other sulfur lines seen by RESIK range from 7.13 to 7.24. The preferred S abundance estimate is close to photospheric and to quiet-Sun solar wind. Described abundance determination method has been also used for the analysis of potassium (K) abundance [23]. Potassium is of importance in the context of FIP effect as the value of FIP for K is very low (4.34 eV). The fluxes of the group of K XVIII lines at 3.53 and 3.57 Å (w, x, y, z including unresolved dielectronic satellites) for 2,795 spectra have been analyzed in this respect. Based on the He-like K resonance line the value of K abundance $A(\mathrm{K}) = 5.86$ with the total range of variability by a factor of 2.9 has been obtained. This is much higher by a factor 5.5 than photospheric abundance estimates, a slightly greater enhancement than for other elements with FIP less than $\sim$10 eV.

The great number of spectra obtained by RESIK spectrometer will be analyzed in future with the purpose of identification of changes of plasma thermodynamic parameters and abundance of elements during individual flares.

Acknowledgements The works with RESIK spectrometer have been carried out with the support of Polish Scientific Research Fund (project 2.P03C.005.08 for technical design; project 1.P03D.017.29 and 2011/01/B/ST9/05861 for data processing).

References

1. Asplund, M., Grevesse, N., Sauval, A.J., Scott, P.: The chemical composition of the Sun. Annu. Rev. Astron. Astrophys. **47**, 481–522 (2009)
2. Culhane, J.L., Hiei, E., Doschek, G.A., Cruise, A.M., Ogawara, Y., Uchida, Y., Bentley, R.D., Brown, C.M., Lang, J., Watanabe, T., Bowles, J.A., Deslattes, R.D., Feldman, U., Fludra, A., Guttridge, P., Henins, A., Lapington, J., Magraw, J., Mariska, J.T., Payne, J., Phillips, K.J.H., Sheather, P., Slater, K., Tanaka, K., Towndraw, E., Trow, M.W., Yamaguchi, A.: The Bragg crystal spectrometer for solar-A. Sol. Phys. **136**, 89 (1991)
3. Dere, K.P., Landi, E., Mason, H.E., Monsignori Fossi, B.C., Young, P.R.: CHIANTI—an atomic database for emission lines. Astron. Astrophys. Suppl. **125**, 149–173 (1997)
4. Feldman, U., Laming, J.M.: Element abundances in the upper atmospheres of the sun and stars: update of observational results. Phys. Scr. **61**, 222–252 (2000)
5. Jakimiec, J., Sylwester, B., Sylwester, J., Serio, S., Peres, G., Reale, F.: Dynamics of flaring loops II. Flare evolution in the density–temperature diagram. Astron. Astrophys. **253**, 269–276 (1992)
6. Kepa, A., Sylwester, J., Sylwester, B., Siarkowski, M., Pillips, K.J.H., Kuznetsov, V.D.: Observations of $1s^2$-1s(np) and 1s-np lines in RESIK soft X-ray spectra. Adv. Space Res. **38**(7), 1538–1542 (2006)
7. Kepa, A., Sylwester, J., Sylwester, B., et al.: Sol. Syst. Res. **40**(4), 294–301 (2006). doi:10.1134/S0038094606040058
8. Mazzotta, P., Mazzitelli, G., Colafrancesco, S., Vittorio, N.: Ionization balance for optically thin plasmas: rate coefficients for all atoms and ions of the elements H to NI. Astron. Astrophys. Suppl. **133**, 403–409 (1998)
9. Phillips, K.J.H., Sylwester, J., Sylwester, B., Landi, E.: Solar flare abundances of potassium, argon and sulphur. Astrophys. J. **589**, 113–116 (2003)
10. Phillips, K.J.H., Dubau, J., Sylwester, B., Sylwester, J., Culhane, J.L., Doschek, G.A., Lang, J.: Temperature-sensitive line ratios diagnostics of the corona based on satellite-to-resonance line ratios of $1s^2$-1s(np) transitions. Adv. Space Res. **38**(7), 1543–1546 (2006)
11. Serio, S., Reale, F., Jakimiec, J., Sylwester, B., Sylwester, J.: Dynamics of flaring loops I. Thermodynamic decay scaling laws. Astron. Astrophys. **241**, 197–202 (1991)
12. Siarkowski, M., Sylwester, J.: The analysis of MG XI ion X-ray spectra obtained from Vertical 9 rocket experiment. Artif. Satellites Space Phys. **20**, 63–70 (1985)
13. Sylwester, J.: Experience of Wrocław team in construction of solar X-ray instruments. ESA SP **493**, 377–382 (2001)
14. Sylwester, J., Farnik, F.: DIOGENESS Soft X-ray spectrometer–photometer for studies of flare energy balance. Astron. Inst. Czech. **41**(3), 149–157 (1990)
15. Sylwester, J., Schrijver, J., Mewe, R.: Multitemperature analysis of solar X-ray line emission. Sol. Phys. **67**, 285–309 (1980)
16. Sylwester, J., Lemen, J.R., Mewe, R.: Variation in observed coronal calcium abundance of X-ray flare plasmas. Nature **310**, 665–666 (1984)
17. Sylwester, B., Sylwester, J., Serio, S., Reale, F., Bentley, R.D., Fludra, A.: Dynamics of flaring loops III. Interpretation of flare evolution in the emission measure-temperature diagram. Astron. Astrophys. **267**, 586–594 (1993)
18. Sylwester, J., Garcia, H.A., Sylwester, B.: Quantitative interpretation of GOES soft X-ray measurements. Astron. Astrophys. **293**, 577–585 (1995)

19. Sylwester, J., Lemen, J.R., Bentley, R.D., Fludra, A., Zolcinski, M.C.: Detailed evidence for flare-to-flare variations of the coronal calcium abundance. Astrophys. J. **501**, 397–407 (1998)
20. Sylwester, B., Sylwester, J., Siarkowski, M., Phillips, K.J.H., Landi, E.: Detection of H- and He-like resonance lines of chlorine in solar flare spectra. Proc. Int. Astronomical Union **2004**(223), 671–674 (2004). Copyright © International Astronomical Union. doi:http://dx.doi.org/10.1017/S174392130400729X
21. Sylwester, J., Gaicki, I., Kordylewski, Z., Kowalinski, M., Nowak, S., Plocieniak, S., Siarkowski, M., Sylwester, B., Trzebinski, W., Bakala, J., Culhane, J.L., Whyndham, M., Bentley, R.D., Guttridge, P.R., Phillips, K.J.H., Lang, J., Brown, C.M., Doschek, G.A., Kuznetsov, V.D., Oraevsky, V.N., Stepanov, A.I., Lisin, D.V.: RESIK: a bent crystal X-ray spectrometer for studies of solar coronal plasma composition. Sol. Phys. **226**(1), 45–72 (2005). doi:10.1007/s11207-005-6392-5
22. Sylwester, B., Sylwester, J., Kepa, A., et al.: Sol. Syst. Res. **40**(2), 125-132 (2006). doi:10.1134/S0038094606020067
23. Sylwester, J., Sylwester, B., Phillips, K.J.H., Kuznetsov, V.D.: Highly ionized potassium lines in solar X-ray spectra and the abundance of potassium. Astrophys. J. **710**, 804–809 (2010)
24. Sylwester, J., Sylwester, B., Phillips, K.J.H., Kuznetsov, V.D.: The solar flare sulphur abundance from RESIK observations. Astrophys. J. **751**, 103–109 (2012)